Journal of Thermal Engineering, Vol. 6, No. 6, Special Issue 12, pp. 312-322, December, 2020
Yildiz Technical University Press, Istanbul, Turkey

EXPERIMENTAL AND NUMERICAL INVESTIGATIONS OF SOLAR FLUX DENSITY DISTRIBUTION OVER FLAT PLATE RECEIVER OF MODEL HELIOSTAT SYSTEM

P. M. Gadhe[1*], S. N. Sapali[2], G. N. Kulkarni[3]

ABSTRACT

The flux density distribution and the temperature of the receiver are important parameters to assess the net thermal energy of any Solar Power Concentrator. In the present work, a heliostat field utilizing ganged type of heliostats for process heating application has been designed. A prototype model of the central receiver system consisting of ganged heliostats has been constructed and installed at Pune, Maharashtra, India. A thermocouple method was used to evaluate the total energy focused by the model heliostat system on a flat receiver. The flux density distribution was validated with the ray tracing simulation software 'SolTrace'. The simulated flux density distribution was found to be in agreement with the measured one for a surface normal error of 10 milliradian. A heliostat field having 100 m^2 total mirror area was designed in the north south cornfield layout. This heliostat field was simulated in 'SolTrace' software by considering the surface normal errors as 10 milliradian and the total energy gain was estimated. For the purpose of simulation to investigate the solar flux falling on the receiver, four days of the year were selected. It includes the March equinox, summer solstice, September equinox, and winter solstice.

Keywords: *Central Receiver System, Ganged Heliostats, Peak Flux, Average Flux, SolTrace*

INTRODUCTION

During the last decade, the utilization of the solar energy gained much attention and thrust because of the radical increase in the price of fossil fuels. Thus many researchers are showing interest in the R&D activities related to this area. As compared to other concentrated solar power techniques, central receiver system has higher concentration ratio. The central receiver system consists of a number of mirrors called as heliostats which are distributed over an area on the ground. These heliostats track the sun continuously and focus the radiation on to the top of tower at the receiver. The solar flux density distribution at the focal plane of the receiver is important term to estimate the energy gain by the central receiver system [1, 2].

There are two techniques, indirect and direct measurement of solar flux on the receiver of the solar concentrating systems. A camera target method is an indirect measurement which offers a high level of spatial resolution of solar flux density distribution. The concentrated solar radiation falling on the receiver, gets reflected from the receiver and is then captured with use of camera, generally with a charge-couple device (CCD) sensor. To estimate the flux density distribution on the receiver an image analysis software is used. Another indirect method is the calorimeter method in which the solar flux is determined by the measurement of heat transfer to a cooling fluid that passes through it. This method is mostly applicable for small scale heliostat field. In the direct measurement method, a flux sensor or the radiometer placed on the receiver directly gives a measurement signal proportional to the irradiative flux [1, 2].

D. L. King et al. [3] experimentally evaluated the heliostat performance of the Central Receiver Test Facility (CRTF) by using a water cooled bar with circular foil heat flux gages to measure the flux density. Strachan et al. [4] tested large area heliostats for flux density distribution by using Beam Characterization system with CCD camera, flux Gauge and image analysis software. Ulmer et al. [5] also used the CCD camera and image analysis software without a flux gauge for measuring the flux density distribution from a dish concentrator. Clifford K et al. [6] determined the flux density distribution by using only CCD camera without requiring the additional sensors, calorimeter or flux gauge. To calibrate the pixel values of CCD image the recorded sun image was used which requires rigorous calculations. In combination with water cooled Lambertian target a thermal infrared imager was used by Xin-LinXia et al. [7] for flux calculation. A flat plate calorimeter was employed by Kretzschmar et al. [8] to measure the flux distribution for small scale heliostat field and requires calculation of heat losses very accurately. Sebastian James Bode et al. [9] used CMOS camera for flux measurement, which is less costly as compared to CCD camera and showing good result. Sebastian-James Bode et al. [10] explored the functionality of the different

This paper was recommended for publication in revised form by Regional Editor Hafiz Muhammed Ali
[1,2]Department of Mechanical Engineering, College of Engineering, Pune, Maharashtra, India
[3]Department of Mechanical Engineering, Government College of Engineering, Chandrapur, Maharashtra, India
**E-mail address: prakash.gadhe@mitpune.edu.in*
Orcid id: 0000-0001-5636-2834, 0000-0002-1326-2937, 0000-0002-0137-2282
Manuscript Received 25 February 2018, Accepted 26 April 2018

codes of software tools used in the optical design, analysis and optimization of central receiver systems. Antonio L. Avila-Marin et al. [11] evaluated the performance of medium to large size central receiver plants based on size and location analysis, technology analysis, storage analysis, components cost analysis. Luis Omar et al. [12] evaluated the optical performance of the Heliostat fieldas a function of the total number of heliostats, the time and date, and the aiming errors by developing a ray tracing model using SolTrace software .T. Kodama et. al. [13] measured the concentrated solar flux at the focus point by moving an array of thirteen Gardon gauges. Hyunjin Lee [14] measured the solar flux with flux mapping method to evaluate optical performance of a solar furnace in the KIER (Korea Institute of Energy Research) and evaluated optical performance in terms of concentrated solar flux distribution and power distribution. All these methods give accurate flux density distribution but these methods are specialized and require costly instruments.

Sharma et al. [15] proposed a thermocouple method which is an indirect and simple flux measurement method. In this method the number of thermocouples were fixed on the back side of the receiver plate. The temperatures on the flat plate receiver in the focal region of the paraboloidal type of dish receiver were measured to estimate the radiation flux and its spatial distribution. C. A. Kinjavdekaret. al. [16] also applied the thermocouple method to estimate the flux density distribution on the flat receiver of Scheffler dish concentrator. Gadhe et. al [17] also employed the thermocouple method for solar flux measurement on the flat plate receiver of small heliostat field.

G. Johnston [18] used video graphic flux mapping to characterize the solar flux distribution of the 400 m^2 solar concentrator, located at the Australian National University. A ray trace code dubbed COMPREC (acronym for COMPound RECeiver) has been written and used for comparison of experimental flux distribution. The technique of surface normal error adjustment was used in the simulation until the modeled and measured distributions showed equal peak intensity. The simulated flux distribution matches with the measured one for a surface normal error of 6 milliradian.

Maurice Maliage et al. [19] used calorimeter method to estimate the solar flux distribution in the focal spot of a 1.25 m^2 target aligned heliostat. The experimental results of flux distribution was validated by using a ray tracing software SolTrace. The results showed that the near-Gaussian shape and radial extent of the flux distribution in the focal spot of the 1.25 m^2 heliostat was well predicted by ray-tracing simulation using SolTrace. Qiang Yu et al. [20] developed a heliostat field model to simulate the solar flux distribution on the inner surfaces of a cavity receiver of a solar tower power plant by means of the Monte-Carlo ray-tracing method. Imhamed M. Saleh Ali et al. [21] used a ray tracing software to evaluate the optical performance of a static 3-D Elliptical Hyperboloid Concentrator (EHC) using ray tracing software.

Alberto Sanchez Gonzalez et al. [22] have given a methodology to project the flux distribution from the image plane into the panels of any central receiver in Solar Power Tower plants. A computer code based on the projection method had been developed and successfully confronted against measurements and SolTrace software, either for flat plate or multi-panel cylindrical receivers. Sasa R. Pavlovic et al. [23] have showed the geometric aspects of the focal image for a solar parabolic concentrator (SPC) using the ray tracing technique to establish parameters that allow the designation of the most suitable geometry for coupling the SPC to absorber-receiver. For optical ray tracing analysis of solar parabolic thermal concentrator software TracePro, Lamda Research Corporation, USA, has been used.

V. Venkatesh et al. [24] developed a dimensionless correlation with respect to tower height and receiver size (diameter and height) as a function of heliostat size and its position in the field. Nicolás C. Cruz [25] had been proposed and described an innovative methodology for data-based analytical characterization of the heliostat field and modelled a whole heliostat field by a reduced set of analytical expressions.

In the present paper, the experimental work, which has been carried out by Gadhe et al. [17] to find the flux density distribution on the receiver of a prototype heliostat field consisting nine heliostats is validated by using the ray tracing software SolTrace. In SolTrace software by varying the surface normal errors such as slope errors and the specularity errors the results were in close agreement with that of experimental results. For the process heating application a heliostat field consisting of total 100 m^2 mirror area was designed. By considering the same slope and secularity errors at which the experimental and the SolTrace results were matching, the designed heliostats field was simulated in SolTrace software and its solar flux distribution was estimated. For the simulation purpose to investigate the solar flux falling on the receiver, four days of the year were selected. These are the March equinox, summer solstice, September equinox, and winter solstice. Based on the flux values on the receiver the steam generation capacity was predicted [27, 28, 29].

EXPERIMENTAL AND NUMERICAL RESULTS

The experimentally estimated flux density distribution is compared with the numerically estimated flux density distribution by using SolTrace software. SolTrace is a Monte-Carlo ray-tracing software package downloadable from the website of the National Renewable Energy Laboratory (NREL) [26]. NREL is a national laboratory of the U.S. Department of Energy.

EXPERIMENTAL RESULTS

Gadhe et al. [17] fabricated a prototype of the heliostat field at location: Pune, India (18.5204^0N, 73.8567^0E), consisting of nine heliostats of size 0.60 m x 0.60 m each and tested for the flux measurement on the flat receiver plate. An Indirect method i. e. the thermocouple method proposed by Sharma and Muley [15, 16] was used for the flux measurement of the heliostat system on the flat receiver. Based on the temperature values measured on the different locations of the flat receiver plate at the thermocouple locations, the flux density distribution on the receiver plate was estimated by using the energy balance equation. Figure 1 shows the photographs of the fabricated prototype heliostat system and the flat receiver plate from different angles. Initially to check the variation of the flux on the receiver plate, the number of heliostats focused on the receiver plate were varied. The flux measurement testing was carried out by focusing a single heliostat near solar noon on the first day. Then the numbers of heliostats were gradually increased such as three, five, six and nine on each day and the flux measurement near solar noon was carried out. For each case the flux density distribution was analyzed and the peak flux and the average flux were estimated.

Figure 1. Heliostat system and the receiver plate [Location: Pune, Maharashtra, India] (photographs from different angle)

NUMERICAL SIMULATION

For the optical analysis of the heliostat system a ray tracing software SolTrace was used. It gives the flux density distribution on the receiver by Monte Carlo ray tracing method. The SolTrace ray tracing software is developed at the National Renewable Energy Laboratory (NREL) in early 2003 and is available for free download at NREL website [26]. To simulate a heliostat system, the SolTrace model requires various inputs. These inputs include: • Location - Date and time; longitude, latitude and altitude, • Heliostats - Heliostat positions in the field, size and shape of heliostats, optical errors, reflectivity of mirrors, • Receiver - Receiver position, shape and size; and optical characteristics

On a particular day and time, the positions of the heliostats with respect to receiver location is to be calculated and the aim points of the heliostats on the receiver plate are to be entered in the SolTrace software. Then on tracing the rays in the software it gives intersection of the rays and the flux map on the receiver plate.The target

position relative to the heliostat was used to obtain the target unit vector. This together with the solar unit vector was used to generate the heliostat normal unit vector. By using the Microsoft excel spread sheet the aiming point unit vectors for all the nine heliostats were calculated and inserted in the ray tracing software SolTrace. The number of rays considered for simulation in SolTrace software were 4 million in the present work. Above 4 million rays the simulation results, such as the peak flux and the average flux values does not show any appreciable change.

The comparison of experimentally and numerically estimated flux (W/m^2) contours of density distribution for one, three, five, seven and nine heliostats at solar noon are shown in Figure 2 (a), (b), (c), (d) and (e) respectively. In these figures the blue colour values denotes the experimental flux values and the red colour values are numerical flux values in W/m^2.

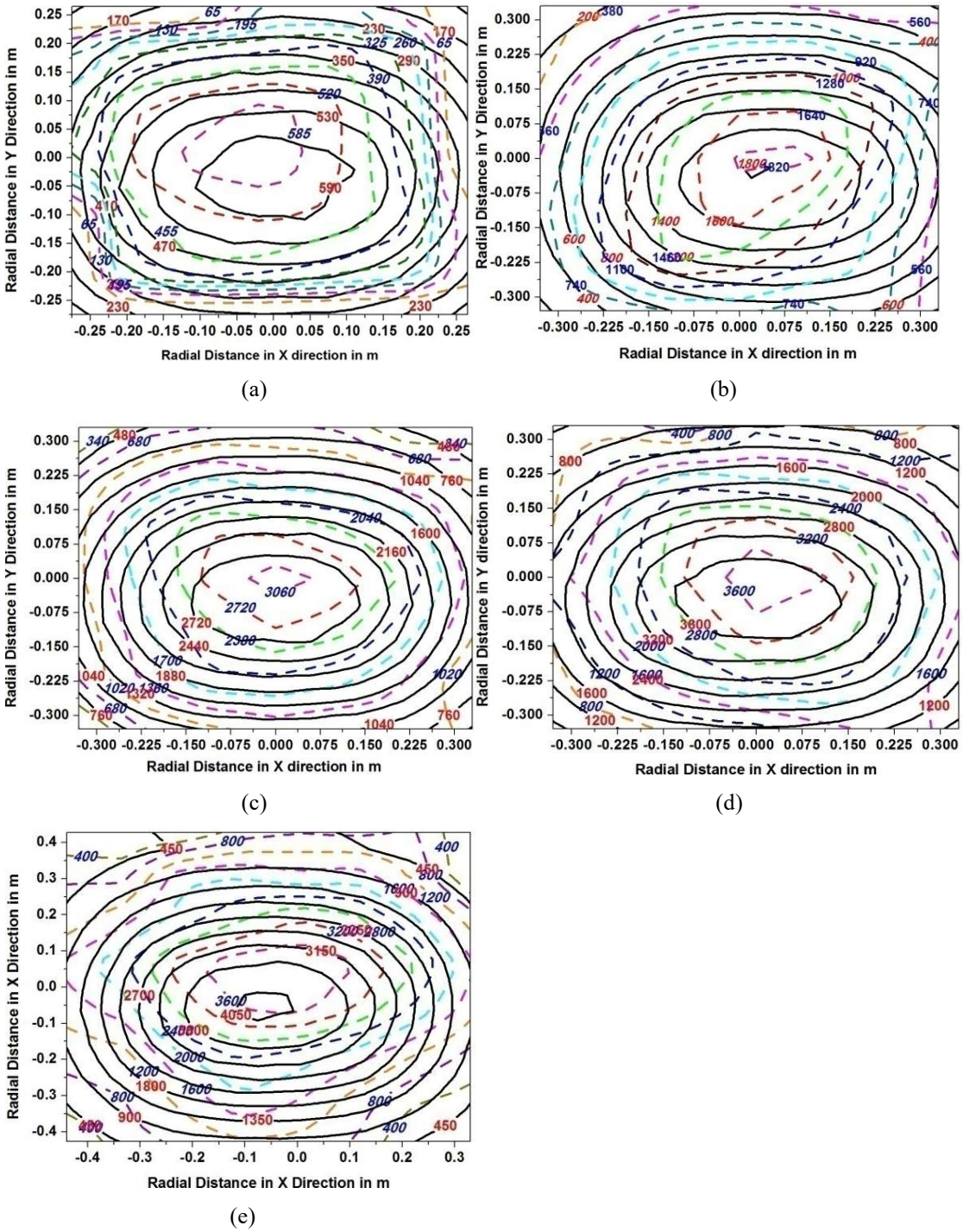

Figure 2. Comparison of experimental (dash lines) and numerical flux (solid lines) (W/m^2) contours on the receiver focusing

The surface normal errors such as slope errors and specularity errors play an important role in the flux density distribution. In SolTrace software during simulation of the heliostat system the slope errors and specularity errors are varied to match with the experimental flux contour maps. It is observed from the simulation results that the SolTrace flux contours are in line with the experimentally calculated flux contours for the slope and specularity errors of 10 milliradian. So from this observation we can say that, the slope errors and the specularity errors are 10 milliradian for the mirrors that is used for this heliostat system. With this slope errors and specularity errors one can simulate the proposed heliostat system in SolTrace software. Table 1 shows the experimentally and numerically calculated peak and average flux values and the percentage errors between them. Figure 3 shows the variation of experimental and numerical values of the peak flux and average flux with the number of heliostats focused.

From Figure 3 it is seen that the numerical flux values are in close agreement with the experimental flux values with the percentage error less than 15%. So to predict the performance of the proposed heliostat system of 100 m^2 mirror area, the SolTrace software was used with the surface normal errors as 10 milliradian.

Table 1. Experimental and numerical peak flux and average flux value

Total Heliostats numbers focused (n)	DNI (W/m^2)	Peak Flux Value (W/m^2)			Average Flux Value (W/m^2)		
		Experimental (± 3.76%)	SolTrace (± 0.76)	% error	Experimental (± 3.76%)	SolTrace (± 0.03)	% error
1	809	637.11	631.49	0.88	380.26	349.49	8.09
3	771	1885.8	1824.24	3.26	942.37	821.88	12.79
5	803	3201.98	2969.22	7.27	1492.78	1411.37	5.45
7	795	3851.1	3898.27	1.21	1852.1	1887.12	1.86
9	710	3950.57	4133.65	4.43	1701.1	1798.77	5.43

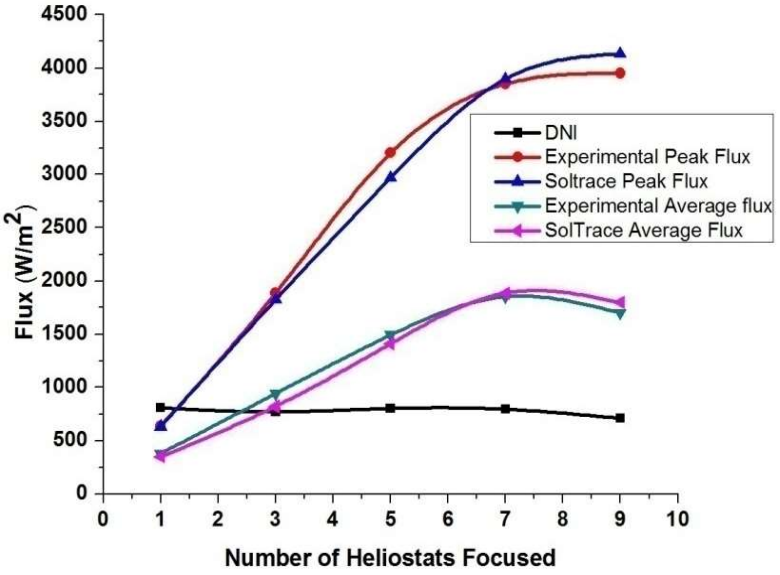

Figure 3. Variation of experimental and numerical values of the peak flux and average flux with the number of heliostats focused

PROPOSED HELIOSTAT SYSTEM

It is required to design the heliostat system for the process heating applications at location: Pune, India (18.52040N, 73.85670E), consisting of the total heliostat mirror area of 100 m^2. As the heliostat system consists of ganged heliostats so the heliostat field is designed for north south configuration. For deciding the azimuthal and radial distance between the heliostats, a radially staggered pattern calculation is incorporated for the north south cornfield configuration. Table 2 gives the design parameters for the heliostat field.

The radial staggered pattern minimizes land usage as well as shadowing and blocking losses. The heliostats are tightly packed near the tower but must be sufficiently separated to prevent mechanical interference [1]. Figure 4 shows the radial stagger heliostat lay out pattern.

Table 2. Design parameter

Sr. No	Parameter	Value
1	Heliostat length (HM)	0.6
2	Heliostat Width (WM)	0.6
3	Heliostat Height from ground (zo)	1
4	Reflective area (Ar)	100 m^2
5	Total Number of Heliostats	277
6	Tower Height (Ht)	4m
7	First row of heliostats from tower	3m (=0.75 x Ht)

The radial spacing ΔR and the azimuthal spacing ΔA, shown in Figure 4 is calculated by using equation 1, 2 and 3 [1].

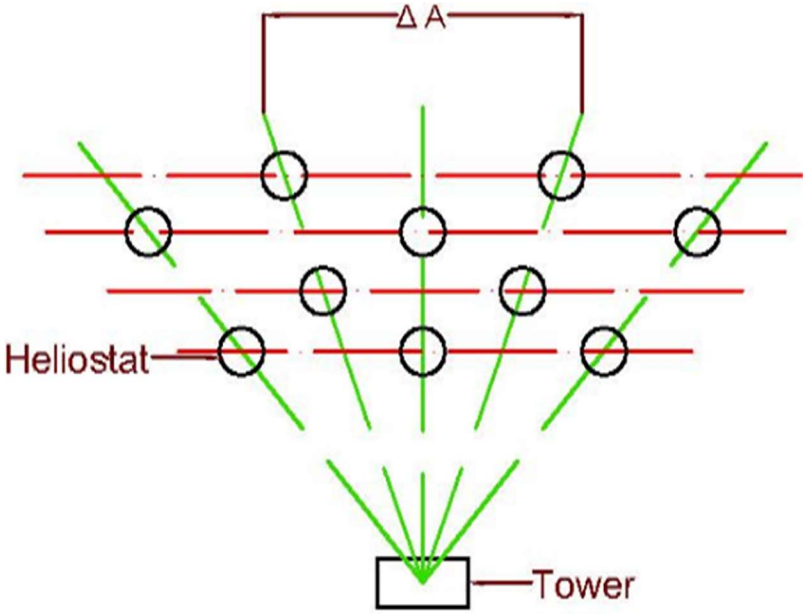

Figure 4. Radial staggered pattern

$$\Delta R = HM\ (1.44\ cot(\theta_L) - 1.094 + 3.068\ (\theta_L) - 1.1256\ (\theta_L^2) \quad (1)$$

$$\Delta R = WM\left(1.749 + 0.6396\ (\theta_L)\right) + \frac{0.2873}{(\theta_L) - 0.04902} \quad (2)$$

$$\theta_L = tan^{-1}\left(\frac{1}{r}\right) \quad (3)$$

Where HM and WM are the height and width of the heliostat and θ_L is the altitude angle of the receiver with respect to heliostats and r is the normalized distance from the tower to the heliostat location measured in "tower heights". Table 3 gives the radial spacing ΔR and the azimuthal spacing ΔA.

Table 3. Radial spacing and azimuthal spacing

Distance of row from the tower (m)	(θ_L) (rad)	Radial spacing (ΔR) (m)	Azimuthal spacing (ΔA) (m)
3.00	0.79	1.75	2.30
4.00	0.66	1.95	2.32
5.00	0.55	2.20	2.36
6.00	0.47	2.51	2.43
7.25	0.39	2.89	2.53
8.75	0.33	3.36	2.68
10.30	0.28	3.95	2.87
12.30	0.24	4.66	3.13
14.75	0.20	5.53	3.47
17.50	0.17	6.59	3.94
20.75	0.14	7.87	4.59
24.00	0.12	9.42	5.53

With the above values of radial spacing ΔR and the azimuthal spacing ΔA for each row of heliostats the heliostat positions in the heliostat field is shown in Figure 5.

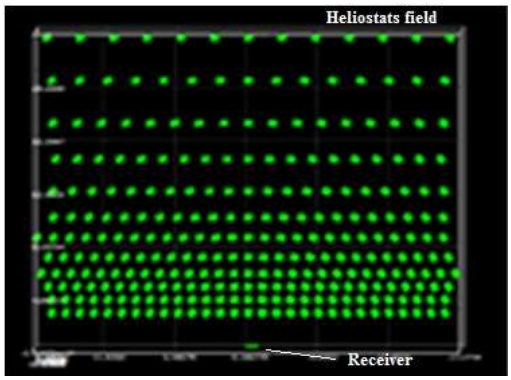

Figure 5. The north south cornfield heliostat layout pattern

This Heliostat field designed was simulated in the SolTrace software with the slope and the specularity error of 10 milliradian. For the simulation in SolTrace software, to investigate the solar flux falling on the receiver four days of the year were selected, these are the March equinox, summer solstice, September equinox, and winter solstice. These periods represent two extreme angles and two middle angles of the year. The Direct Normal Irradiance (DNI) values for these four days are presented in Figure 6.

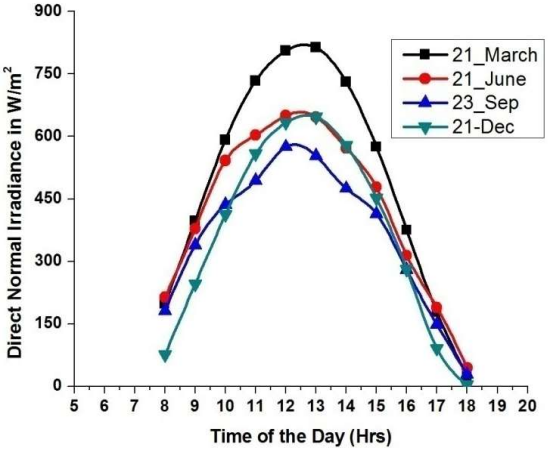

Figure 6. Variation of DNI values

The overall distribution of flux density on the receiver from the heliostat field of 277 heliostats has been evaluated in SolTrace software. The number of rays considered for simulation in SolTrace software were 4 million. All the heliostats were aimed at the receiver centre. The solar flux density contour on the receiver at the solar noon on the March equinox day is shown in Figure 7 with flux values in W/m^2.

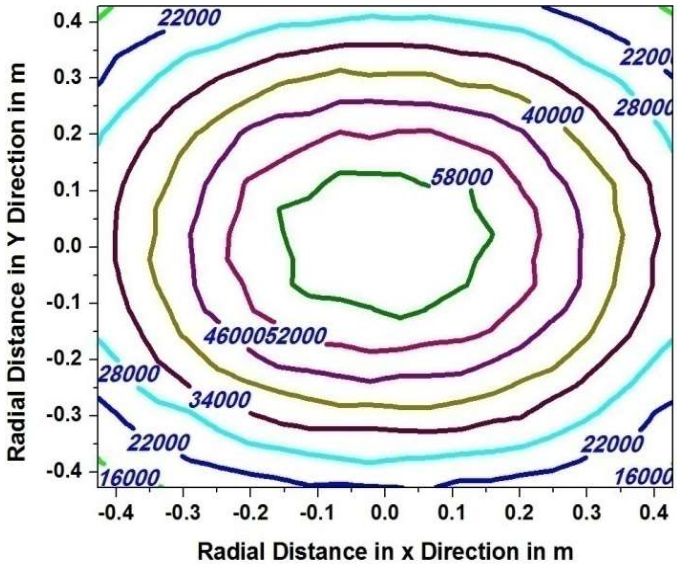

Figure 7. SolTrace flux (W/m^2) contours on the receiver

Figure 8 represents the changes in the energy falling on the receiver throughout the day during the March equinox, summer solstice, September equinox, and winter solstice. The maximum energy falling on the receiver was detected during the March equinox, while the lowest values was found during the September equinox. This kind of variation occurs because of the variation of Direct Normal Irradiance (DNI) value due to changing position of the sun throughout the year. Moreover, the solar flux first increases to a maximum value at solar noon and subsequently decreases during the remainder of the day. The highest solar flux value during the March equinox, summer solstice, September equinox, and winter solstice are 37.61, 28.91, 26.63 and 30.03 kW/m^2, respectively.

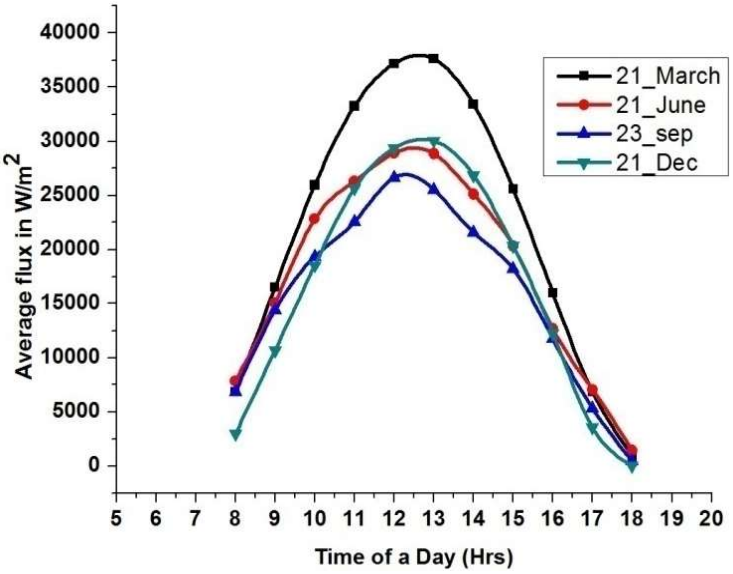

Figure 8. Variation of average flux values on the receiver

Based on the values of the solar flux energy falling on the receiver by the heliostat field, as the heliostat system is to be used for process heating applications, the steam generation was estimated for the same four days of the year. A sample calculation of the steam generation for the spring equinox at 13.00 Hr. is shown in the table 4.

Table 4. The energy yield & steam generation

Area of single heliostat (*A*= 0.6m x 0.6m)	0.36	m^2
Total Mirror area required (*Amt*)	100	m^2
Total Number of heliostats in the field (*Amt* /*A*)	277	
Direct Normal irradiance (I_B)	813.95	W/m^2
Energy on the Receiver= Q_R	37175.30	W/m^2
Total Energy on receiver = Q_R x *Receiver Area* *Receiver Area is considered as 1 m^2	37175.30	W
Total Energy in J/hr, $E_R = Q_R$ x 3600	133.83	MJ/hr
Energy in kcal= $Q = E_R \div 4200$	31864.54	kcal/hr
Energy utilization for steam generation, $E_S = Q$ * *heat Loss coefficient* (14%)	27403.50	kcal/hr
1 Boiler Horse Power (*BHP*)	8436	kcal/hr
BHP Required = $E_S \div BHP$	3.24	kcal/hr
for 1*BHP* steam generation rate	15.65	kg of steam/hr
Therefore for 3.604 *BHP* steam generation rate	50.83	kg of steam/hr

Figure 9 depicts the changes in the steam generation estimated due to energy falling on the receiver throughout the day based on above calculations shown in Table 4, during the March equinox, summer solstice, September equinox, and winter solstice. The steam generation rate becomes maximum near the solar noon. The maximum values of steam generation during the March equinox, summer solstice, September equinox, and winter solstice are 50.83, 39.53, 36.42, 40.15 kg of steam per hour respectively.

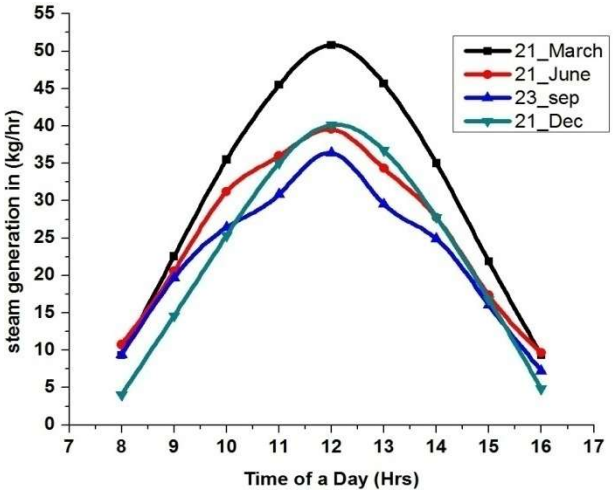

Figure 9. Variation of steam generation

CONCLUSIONS

A Monte Carlo ray tracing software SolTrace was used for validating the experimental results of flux measurement of the prototype model heliostat system. Based on the experimental and numerical simulation following conclusions were made

1. The SolTrace flux contours are in close agreement with the experimentally calculated flux contours for the slope and specularity errors of 10 milliradian. Based on this observation it is seen that, the slope errors and the specularity errors are 10 milliradian for the mirrors that were used for the heliostat system.
2. It is observed that the numerical flux values are nearly matching to that of the experimental flux values with the percentage error of less than 15%.

3. The highest solar flux value given by the presently designed heliostat field during the March equinox, summer solstice, September equinox, and winter solstice evaluated using SolTrace simulation are 37.61, 28.91, 26.63 and 30.03 kW/m^2, respectively.
4. The maximum values of steam generation estimated based on average flux values during the March equinox, summer solstice, September equinox, and winter solstice are 50.83, 39.53, 36.42, 40.15 kg of steam /hr respectively.
5. The present heliostat system would be used for process heating applications, wherein it can be shown that the steam generation throughout the year changes from 5 kg of steam pear hour to around 50 kg of steam per hour due to the variation of solar radiation.
6. The present heliostat system is a ganged type of heliostat system and east west mounted heliostats in straight line. To improve the performance of the present system the heliostat should be mounted in curvature which may be the future scope.

ACKNOWLEDGEMENTS

The authors gratefully acknowledge the contribution and the facility provided by the Maharashtra Institute of Technology, Kothrud, Pune, India and Dr. Ravindra Patwardhan and M. D. Akole, from Akson Solar Equipment Private ltd., Bhor, Pune, India. The authors would also like to acknowledge the Board of College and University Development (BCUD), Savitribai Phule Pune Univeristy for providing financial support to this research work.

REFERENCES

[1] Geyer M, Stine WB. Power from the Sun (Powerfromthesun.net). JT Lyle Center. 2001. (Accessed 1 April 2013).
[2] Ballestrín J, Burgess G, Cumpston J. Heat flux and high-temperature measurement technologies for concentrating solar power (CSP). Concentrating solar power technology-developments and applications. Ed. K Lovegrove and W Stein. (Woodhead Publishing, 2012, 3-15).
[3] King DL, Arvizu DE. Heliostat characterization at the central receiver test facility.
[4] Strachan JW, Houser RM. Testing and evaluation of large-area heliostats for solar thermal applications. Sandia National Labs., Albuquerque, NM (United States); 1993 Feb 1.
[5] Ulmer S, Reinalter W, Heller P, Lu¨ pfert E, Martinez D. Beam characterization and improvement with a flux mapping system for dish concentrators. InInternational Solar Energy Conference 2002 Jan 1 (Vol. 16893, pp. 285-292).
[6] Ho CK, Khalsa SS. A flux mapping method for central receiver systems. InEnergy Sustainability 2011 Jan 1 (Vol. 54686, pp. 743-751).
[7] Xia XL, Dai GL, Shuai Y. Experimental and numerical investigation on solar concentrating characteristics of a sixteen-dish concentrator. International journal of hydrogen energy. 2012 Dec 1;37(24):18694-703.
[8] Kretzschmar H, Gauche P, Mouzouris M. Development of a flat-plate calorimeter for a small-scale heliostat field. SolarPaces, Marrakech, Morocco. 2012 Sep:11-4.
[9] Bode S, Gauche P, Landman W. The design and testing of a small scale solar flux measurement system for central receiver plant. InCRSES Annual Student Symposium 2012.
[10] Bode SJ, Gauché P. Review of optical software for use in concentrating solar power systems. InProceedings of South African Solar Energy Conference 2012 May 21.
[11] Avila-Marin AL, Fernandez-Reche J, Tellez FM. Evaluation of the potential of central receiver solar power plants: configuration, optimization and trends. Applied energy. 2013 Dec 1;112:274-88.
[12] Cerecedo LO, Pitalua-Diaz N, Transito IS, Contreras LE, Bulnes CA. Optical performance modeling of a solar tower heliostat field and estimation of receiver temperature. In2013 IEEE International Autumn Meeting on Power Electronics and Computing (ROPEC) 2013 Nov 13 (pp. 1-6). IEEE.
[13] Kodama T, Gokon N, Matsubara K, Yoshida K, Koikari S, Nagase Y, Nakamura K. Flux measurement of a new beam-down solar concentrating system in Miyazaki for demonstration of thermochemical water splitting reactors. Energy Procedia. 2014 Jan 1;49:1990-8.
[14] Lee H, Chai K, Kim J, Lee S, Yoon H, Yu C, Kang Y. Optical performance evaluation of a solar furnace by measuring the highly concentrated solar flux. Energy. 2014 Mar 1;66:63-9.

[15] Sharma VR, Bhosale SJ, Kedare SB, Nayak JK. A simple method to determine optical quality of paraboloid concentrating solar thermal collector. SESI Journal: Journal of the Solar Energy Society of India. 2005 Dec 1;15(2):21.
[16] Kinjavdekar CA, Muley VP, Kedare SB, Nayak JK. A Test Procedure for Determining Optical characteristics of a Dish Concentrator and its Implementation on Scheffler Dish. SESI Journal. 2010 Dec;20(1):13-23.
[17] Gadhe P, Ghoti A, Sapali S, Kulkarni G. Experimental Method to Find the Flux and Temperature Distribution on the Flat Receiver of Small Central Receiver System. International Review of Mechanical Engineering (IREME). 2017;11(6):426.
[18] Johnston G. Flux mapping the 400 m2 "Big Dish" at the Australian National University.
[19] Maliage M, Roos TH. The flux distribution from a 1.25 m2 target aligned heliostat: comparison of ray tracing and experimental results.
[20] Yu Q, Wang Z, Xu E, Zhang H, Lu Z, Wei X. Modeling and simulation of 1 MWe solar tower plant's solar flux distribution on the central cavity receiver. Simulation Modelling Practice and Theory. 2012 Dec 1;29:123-36.
[21] Ali IM, O'Donovan TS, Reddy KS, Mallick TK. An optical analysis of a static 3-D solar concentrator. Solar Energy. 2013 Feb 1;88:57-70.
[22] Sánchez-González A, Santana D. Solar flux distribution on central receivers: A projection method from analytic function. Renewable Energy. 2015 Feb 1;74:576-87.
[23] Pavlovic SR, Stefanovic VP. Ray tracing study of optical characteristics of the solar image in the receiver for a thermal solar parabolic dish collector. Journal of Solar Energy. 2015 Oct 29;2015.
[24] Venkatesh V, Rao BS, Srilakshmi G, Thirumalai NC, Ramaswamy MA. Correlation between central receiver size and solar field using flat heliostats. Applied Solar Energy. 2017 Jul 1;53(3):258-66.
[25] Cruz NC, Álvarez JD, Redondo JL, Fernández-Reche J, Berenguel M, Monterreal R, Ortigosa PM. A new methodology for building-up a robust model for heliostat field flux characterization. Energies. 2017 May;10(5):730.
[26] http://www.nrel.gov/csp/soltrace/download.htm, (Accessed 2 June 2016).
[27] Hoffmann J. Testing and analysis of low pressure, transparent tube solar receiver for the sunspot cycle. Journal of Thermal Engineering. 2017 Jul 1;3(3):1294-307.
[28] Balotaki HK. Experimental investigation of dual-purpose solar collector using with rectangular channels. Journal of Thermal Engineering. 2017 Jan 1;3(1):1052-9.
[29] Kerme E, Kaneesamkandi Z. Performance analysis and design of liquid based solar heating system. Journal of Thermal Engineering. 2015 Feb 1;1(5):182-91.